

1 **Transient photoreception in the hindbrain is permissive to the life history transition of**
2 **hatching in Atlantic halibut**

3

4 Mariann Eilertsen, ^{1*} Ragnhild Valen, ^{1**} Øyvind Drivenes, ^{2***} Lars O.E. Ebbesson, ^{1,3} and
5 Jon Vidar Helvik ¹

6

7 ¹ Department of Biological Sciences, University of Bergen, N- 5020 Bergen, Norway

8 ² Department of Molecular Biology, University of Bergen, N- 5020 Bergen, Norway

9 ³ Uni Research AS, Thormøhlensgt. 55, N-5008 Bergen, Norway

10

11 Abbreviated title: Transient photoreception permits hatching

12

13 * Corresponding author and reprint request to:

14 Mariann Eilertsen, Department of Biological Sciences, University of Bergen, P.O Box 7803,
15 N- 5020 Bergen, Norway, Mariann.Eilertsen@uib.no

16

17 ** Current address: The Sars International Centre for Marine Molecular Biology, University
18 of Bergen, N- 5020 Bergen, Norway

19

20 *** Current address: Bergen University College, N- 5020 Bergen, Norway

21

22 Declarations of interests:

23 None

24

25 Support: The study was supported by the University of Bergen (Startup package (JVH)) and
26 The Research Council of Norway, Project number 254894 (Havbruk2). The funding source
27 had no involvement in the study design, collection of data, analysis and interpretation of data,
28 writing of the report and the decision to submit the article for publication.

29

30

31

32

33

34

35 **Abstract**

36 In nonmammalian vertebrates, photoreception takes place in the deep brain already early in
37 development, but knowledge is lacking about the functions of these nonvisual photoreceptive
38 systems. Prior to hatching, Atlantic halibut has a transient bilateral cluster of photoreceptive
39 cells in the hindbrain. The cluster is imbedded in a neuronal network projecting to the narrow
40 belt of hatching glands in the yolk sac. In halibut, hatching is inhibited in light and activated
41 by transfer to darkness and *c-fos* analysis during hatching shows that the hindbrain cluster and
42 hatching glands have neural activation. Unexpectedly, the hindbrain cluster expresses dual
43 photopigments, vertebrate ancient opsin and melanopsin. Evolutionarily, these opsins are
44 believed to belong to different classes of photopigments found in rhabdomeric and ciliary
45 photoreceptors. The concept that an organism develops transient light sensitivity to target
46 critical aspects of life history transitions as hatching provides a fascinating landscape to
47 investigate the timing of other biological events.

48

49 Keywords: nonvisual photoreceptor, melanopsin, vertebrate ancient opsin, *c-fos*,

50

51

52

53

54

55

56

57

58

59

60

61

62

63

64

65

66

67

68

69 **Introduction**

70 Light detection is essential for most animals to coordinate behavioral and physiological
71 processes with photic cues. Photoreception is often related to sensory organs such as the retina
72 and pineal, which provide vision and photic information to the animal throughout life. New
73 complexities to this system have appeared in the last decade as new photoreceptor families
74 have been identified with expression outside the classical photoreceptor areas such as within
75 the deep brain (Peirson et al., 2009; Davies et al., 2010; Fernandes et al., 2013; Davies et al.,
76 2015).

77

78 There is a considerable knowledge gap between location and function of deep brain
79 photoreceptor cells. Until now, many photoreceptive cells and their photosensitive pigments
80 have been identified, but how they contribute to light driven behavioral and physiological
81 responses is just emerging. In unhatched zebrafish embryos photoreceptors in the hindbrain
82 are responsible for a “photomotor response” after exposure to intense light (Kokel et al.,
83 2013) and zebrafish larvae lacking eyes and pineal organs demonstrate a light seeking
84 behavior triggered by loss of illumination. Melanopsin-expressing cells in the preoptic area
85 were found to regulate this light seeking behavior (Fernandes et al., 2012). Further, it has been
86 shown that inter- and motoneurons co-express tissue multiple tissue opsin (tmt-opsin) and
87 vertebrate ancient opsin (VA opsin) in zebrafish and medaka brain. Light sensitivity in inter-
88 and motoneurons is suggested to represent a fast possibility to adapt behavior to
89 unpredictable environmental light changes, independent of neurosecretory cells (Fischer et al.,
90 2013). In masu salmon key genes regulating seasonal reproduction and opsins are expressed
91 in the coronet cells of the saccus vasculosus and it has been suggested to be a seasonal sensor
92 in fish sensing changes in day length (Nakane et al., 2013). The marine flat fish Atlantic
93 halibut has a special early life strategy with light-regulated hatching at an early developmental
94 stage long before the eyes are functional (Helvik and Walther, 1992). In Norwegian coastal
95 waters, the halibut spawns in the deep sea and the eggs ascend in the water column to 100-250
96 meters depth, where the hatching process takes place (Haug, 1990; Haug et al., 1984). In the
97 dark winter season, the eggs are only exposed to low light intensities deep in the sea.

98

99 The aim of this study was to unravel the enigma of how light can regulate hatching in halibut
100 and determine if and how deep brain photoreceptor systems are involved in this early life
101 history transition. Previous studies on the hatching mechanism in halibut have demonstrated
102 in detail the effect of the sensory input from the environment (Helvik et al., 1991; Helvik and

103 Walther, 1992; 1993). Light serves as a natural cue for hatching in halibut and halibut larvae
104 in nature hatch in darkness (Helvik and Walter, 1992). Further, the hatching glands are
105 located in a narrow belt in the yolk sac and during hatching the yolk sac is reshaped by
106 contraction so that the yolk mass is squeezed anterior before hatching. This ensures close
107 contact between the hatching glands and the eggshell during release of the hatching enzyme,
108 which is necessary for restricted degradation of the eggshell (Helvik et al., 1991). The pineal
109 has been proposed to be important in perceiving and mediating photic information in the
110 hatching process (Forsell et al., 1997), however a connection between the pineal and hatching
111 is still missing. We have revealed diverse photopigment expression patterns in the brain and
112 spinal cord early in development of Atlantic halibut, indicating that other photosensitive
113 regions also may be important in hatching (Eilertsen et al., 2014). From an evolutionary point
114 of view, the nonvisual pigments are of interest since they belong to two different classes of
115 photopigments, melanopsin, as r-opsin, and vertebrate ancient opsin (VA opsin), as c-opsin,
116 normally only found in rhabdomic and ciliary photoreceptor cells, respectively. The
117 evolutionary origin of photoreceptor cell types is still debated (Davies et al., 2010; Matos-
118 Cruz et al., 2011; Vocking et al., 2017), with the theory of ancient photoreceptors containing
119 duplicated photopigments that subsequently became distinct receptor cells expressing c- and
120 r-opsin (Arendt, 2003). Strikingly, we found a cluster of cells in the hindbrain of Atlantic
121 halibut expressing transiently both melanopsin and VA opsin. This cluster of dual
122 photoreceptors is imbedded in a neuronal network with fibers proceeding out in the yolk sac,
123 reaching the hatching gland cells. Studies with photo-arrested eggs demonstrate that dark
124 induced hatching activates the immediate early gene *c-fos* in the hindbrain cluster and in the
125 hatching glands. Taken together, our data imply how an early life history transition is
126 modulated by transient and direct photoreception in the brain.

127

128 **Materials and methods**

129

130 **Animals.** Eggs of Atlantic halibut (*Hippoglossus hippoglossus*) were obtained from the
131 Institute of Marine Research, Austevoll Aquaculture Station, Norway. All experiments
132 described follow the local animal care guidelines and were given ethical approval by the
133 Norwegian Veterinary Authorities.

134

135 **Molecular cloning of vertebrate ancient opsin.** Total RNA was isolated from the retina and
136 brain of juvenile Atlantic halibut by Trizol reagent (Life Technologies, Bethesda, MD).

137 Purification of Poly A⁺ mRNA was carried out with Oligotex Resin (Qiagen, Germany) and
138 preparation of double stranded cDNA and adaptor-ligated cDNA were done using Marathon
139 cDNA Amplification Kit (Clontech, Palo Alto, CA). Isolation of VA opsin in halibut was
140 done by PCR using degenerative primers as described in Helvik et al. (2001). To generate
141 full-length of the gene, Rapid Amplification of cDNA Ends (RACE) was done with a nested
142 approach. In the first round with 35 cycles, the annealing temperature was 62.9°C for
143 5'RACE and 60°C for 3'RACE. The second round of PCR had an annealing temperature of
144 66.5°C for both 5' and 3' RACE and 35 cycles were used. The nested 3'RACE resulted in
145 two PCR products of different length and the assembly of the two RACE products was
146 verified by a PCR with primer binding sites located in the predicted the 5' and 3' UTRs. The
147 two isoforms are identical in the four first exons, but the fifth exon is altered in the two
148 isoforms as in zebrafish (Kojima et al., 2000) and provides different length in the cytoplasmic
149 tail. As shown in chicken (Halford et al. 2009) the short isoform of VA opsin is generated by
150 a read-through into intron 4 while the long isoforms by splicing to exon 5. PCR products were
151 extracted from agarose gel using QIAEX II Gel Extraction Kit (Qiagen, Germany) or
152 MinElute[®]Gel Extraction Kit (Qiagen, Germany) before cloning into StrataClone PCR
153 Cloning vector pSC-A-amp/kan (Agilent Technologies, LA Jolla, CA) or pGEMT[®]-Easy
154 Vector (Promega, Madison, WI) and sequencing at the University of Bergen Sequencing
155 Facility. Primers are listed in Table 1. The nucleotide sequences were deposited into
156 GeneBank with the accession number KF941295 (*val*) and KF941296 (*vas*).

157
158 **Verification of VA opsin and identification of *c-fos*.** The halibut genome has recently been
159 sequenced on an Illumina HiSeq200 (Illumina, San Diego, CA) (Pair End, 100bp reads) to
160 40x coverage and a contig assembly has been made by the CLC software (CLC bio, Denmark,
161 RRID: OMICS_01124). The genome was searched by BLASTN and TBLASTN (NCBI,
162 Bethesda, MD, RRID: nlx_153932 and RRID: OMICS_00999) with the two isoforms of VA
163 opsin to verify the sequence obtained by PCR. In addition the genome was searched by
164 TBLASTN using available teleost protein opsin sequences as a query in order to obtain a
165 potential duplicate of VA opsin as seen in zebrafish (Kojima et al., 2008). For *c-fos* the
166 genome was searched by TBLASTN using available teleost C-fos protein sequences as query
167 in order to obtain the sequence of the gene in halibut. The putative gene was predicted based
168 on the BLAST alignments and GENSCAN (Burge and Karlin, 1997), and the annotation was
169 based on BLASTX (NCBI, Bethesda, MD, RRID: nlx_153933) against GenBank (NCBI,
170 Bethesda, MD, RRID: nif-0000-02873) and phylogenetic analysis. Verification of the

171 predicted gene was done by PCR using primers with binding sites in the predicted 5' and 3'
172 UTR and cloning and sequencing was done as for VA opsin. The nucleotide sequence for *c-*
173 *fos* was deposited into GeneBank with the accession number KF941297.

174

175 **Riboprobes.** Preparation of digoxigenin (DIG)-labelled and fluorescein-labelled riboprobes
176 for VA opsin (specific for both isoforms) and DIG-labelled riboprobe for melanopsin
177 (*opn4m3*) (specific for both isoforms) and *c-fos* were done following the manufacturer's
178 instructions (Roche Diagnostics, Germany). In the synthesis of the riboprobes PCR product
179 was used as template for the reaction as described in Thisse and Thisse (2008) and the
180 synthesized probes were precipitated by LiCl and EtOH together with tRNA (Roche
181 Diagnostics, Germany). Sequence alignment showed that the similarity between the sequence
182 targets of the melanopsin and VA opsin probes is approximately 50% (data not shown),
183 ensuring no cross-hybridization. Sequence information is listed in Table 2.

184

185 ***In situ* hybridization (ISH).** ISH on whole embryos and larvae of different developmental
186 stages was done as described in Eilertsen et al. (2014) using DIG-labelled riboprobe for VA
187 opsin, melanopsin and *c-fos*. Color staining was performed by 4-Nitro blue tetrazolium
188 chloride and 5-Bromo-4-chloro-3-indolyl-phosphate system (Roche Diagnostics, Germany).
189 ISH on cryosections (12 and 13 days post fertilization (dpf)) was performed following the
190 preparations and ISH protocol described in Sandbakken et al. (2012). Briefly, the embryos
191 were embedded in Tissue-Tek O.C.T. Compound (Sakura Fintek, Netherlands) and sectioned
192 (10 µm) on a Leica CM 1850 cryostat (Leica Microsystems, Germany). Prior to the
193 hybridization step the tissue was rehydrated in ethanol, permeabilized with proteinase K and
194 treated with triethanolamine (Sigma, St. Louis, MO) and acetic anhydride (Sigma, St. Louis,
195 MO) to reduce background staining. After hybridization the tissue was thoroughly washed
196 and treated with RNase A (Sigma, St. Louis, MO) to remove unhybridized probe. Before
197 applying the antibody (anti-digoxigenin conjugated with alkaline phosphatase, Fab fragments
198 (1:2000) (Cat. No 11093274910, Roche Diagnostics, Germany, RRID: AB_514497)) the
199 tissue was incubated in 2% blocking solution (Roche Diagnostics, Germany) in 2x SSC with
200 0.05% Triton X-100 (Sigma, St. Louis, MO). The DIG-labelled probe was visualized by 4-
201 Nitro blue tetrazolium chloride and 5-Bromo-4-chloro-3-indolyl-phosphate system (Roche
202 Diagnostics, Germany). Parallel sections were Nissl-stained with 0,5% cresyl fast violet
203 (Chroma-Gesellschaft, Germany).

204

205 **Fluorescent double labelling ISH.** Fluorescent double labelling ISH on cryosections (12 dpf)
206 was performed following the preparations and ISH protocol described in Sandbakken et al.
207 (2012), except that both probes were applied at the hybridization step. In addition, the
208 fluorescein-labelled riboprobe for VA opsin was first visualized by using the antibody anti-
209 fluorescein conjugated with horse radish peroxidase, Fab fragments (1:400) (Cat. No
210 11426346910, Roche Diagnostics, Germany, RRID: AB_840257) and the TSATMPlus
211 Fluorescein Systems (Perkin Elmer, Waltham, MA) according to the producer's protocol.
212 Before applying anti-digoxigenin conjugated with alkaline phosphatase, Fab fragments
213 (1:2000) (Cat. No 11093274910, Roche Diagnostics, Germany, RRID: AB_514497) the
214 sections were blocked for 1 hour in 2% Blocking reagent (Roche Diagnostics, Germany) in
215 2xSCC, and the DIG-labelled riboprobe for melanopsin was visualized by use of Fast Red
216 tablets as recommended by the manufacturer (Roche Diagnostics, Germany). The stained
217 sections were mounted in DABCO antifading medium (Sigma, St. Louis, MO). Fluorescent
218 double labelling ISH on whole embryos was done as described in Eilertsen et al. (2014).
219 Fluorescein-labelled riboprobe for VA opsin was visualized with the TSATMPlus Fluorescein
220 System and the DIG-labelled probe for melanopsin or *c-fos* was visualized with Fast Red
221 tablets.

222

223 **Immunohistochemistry.** To evaluate the neuronal fiber network at the stage of hatching,
224 immunohistochemistry on whole embryos (13 dpf) with monoclonal anti-acetylated tubulin
225 antibody produced in mouse (Clone 6-11 B-1) (1:1000) (Cat. No T7451, Roche Diagnostics,
226 Germany, RRID: AB_609894) was done as described in Eilertsen et al. (2014), except for the
227 following modifications. The embryos were incubated in monoclonal anti-acetylated tubulin
228 antibody overnight at room temperature and for visualization anti-mouse IgG (H+L), CFTM
229 488A antibody produced in goat 2 mg/ml (Cat.No SAB4600042, Sigma-Aldrich, St. Louis,
230 MO, RRID: AB_2532075) was used.

231

232 **ISH and immunohistochemistry in combination.** The combination of ISH and
233 immunohistochemistry on whole halibut embryo (13 dpf) was performed as explained in
234 Eilertsen et al. (2014). Fluorescein-labelled riboprobe was used for VA opsin and the probe
235 was visualized by TSATMPlus Fluorescein Systems (Perkin Elmer, Waltham, MA).
236 Monoclonal anti-acetylated tubulin antibody produced in mouse (Clone 6-11 B-1) (1:1000)
237 (Cat. No T7451, Roche Diagnostics, Germany, RRID: AB_609894) and anti-mouse IgG
238 (H+L), CFTM 555 antibody produced in goat 2 mg/ml (1:100) (Cat. No SAB4600066, Sigma-

239 Aldrich, St. Louis, MO, RRID: AB_2336060) were used for staining of neuronal fiber
240 network.

241

242 **Antibody characterization.** Mouse anti-acetylated tubulin (Cat. No. T7451, Sigma-Aldrich,
243 St. Louis, MO, RRID: AB_609894) is a monoclonal antibody that recognizes an epitope
244 located on the $\alpha 3$ isoform of *Chlamydomonas axonemal* α -tubulin. The antibody has been
245 shown to recognize a single 55 kDa band (the predicted molecular weight of acetylated
246 tubulin) on western blots of teleost brain extracts (Liu and Lessman, 2007). In addition, the
247 antibody has also been shown to specifically label axons in the developing central nervous
248 system of zebrafish (Chitnis and Kuwada, 1990). The antibody has been used to label axons in
249 many organisms including teleosts (Ledizet and Piperno, 1991; Hunter et al., 2011; Verpy et
250 al., 2011). See Table 3 for details.

251

252 **Functional studies with photo-arrested eggs.** The functional studies with photo-arrested
253 eggs were set up based on the knowledge of a dark-induced hatching process in Atlantic
254 halibut. Incubation in light arrests the hatching mechanism but if photo-arrested eggs are
255 placed in darkness after their natural hatching point, they will hatch in synchrony and rapidly
256 within 80-140 minutes (Helvik and Walther, 1992). To investigate a possible neuronal
257 regulation of hatching, eggs were placed in light (MASTER PL-S 11W/827/2P 1CT, Philips
258 Lighting, Netherlands) before they reached the natural hatching point. The photo-arrested
259 eggs were transferred to darkness at 18 dpf, a time point after the natural hatching point, to
260 induce the dark-dependent hatching signal. Eggs were sampled by putting them in ice-cold
261 4% paraformaldehyde after 2, 10, 20, 30, 40, 60 and 120 minutes in the dark. The experiment
262 was conducted using night vision device (Bushnell, Overland Park, KS), to minimize the light
263 exposure upon sampling. In addition, eggs incubated in light were used as a control. To mark
264 neuronal activation ISH with DIG-labelled riboprobe for *c-fos* was done for all the points
265 sampled including the control kept in light.

266

267 **Pictures of living halibut embryos.** Living embryos (16 dpf) in eggshell were mounted in
268 3% methylcellulose (Sigma-Aldrich, St. Louis, MO) and oriented in a dorsal and lateral view.
269 Photo-arrested eggs in sea-water (18 dpf) were transferred to darkness to induce hatching and
270 pictures were taken using a Leica M420 macroscope (Leica Microsystems, Germany) and a
271 CoolSNAP-Pro Color Imaging Camera (RS Photometrics, Tucson, AZ).

272

273 **Microscopy and photographic manipulation.** Pictures were taken by using a digital camera
274 Leica DFC 320/ Leica 350 FX (Leica Microsystems, Germany) attached to a Leica DM
275 6000B microscope (Leica Microsystems, Germany) with an ebx75mc-L90 lamp
276 (Leistungselektronik Jena GmbH, Germany). Confocal images were taken using the Leica
277 TCS SPE confocal system together with a Leica DM2500 microscope (Leica Microsystems,
278 Germany). Confocal imaging of acetylated alpha tubulin was done using a Zeiss LSM 510
279 Meta with 10x Plan-Neofluar 0,3 NA or 20x Plan-Neofluar 0,5 NA (Zeiss, Germany) and the
280 pictures were generated merging a stack of pictures providing a 3D projection. A movie of the
281 pictures from the 3D projection and a movie of different focal levels were also made (See
282 Supplementary Figure 4 and 5). All pictures of the fluorescent double labelling with VA opsin
283 and melanopsin (fluorescent and confocal imaging) are single pictures with one focus plane
284 and not a stack of pictures with different focus planes merged together. Adobe Photoshop CS5
285 (San Jose, CA) was used for adjustments of brightness, contrast, color levels and to sharpen
286 the pictures.

287

288 **Results**

289

290 **Transient and dual expression of vertebrate ancient opsin and melanopsin in the**
291 **hindbrain at the time of hatching.** The halibut eggs are known to hatch at an early
292 developmental stage when the larvae are transparent and the retina consists of neuroblastic
293 cells (Haug, 1990; Kvenseth et al., 1996). Figure 1A, C-D show a living halibut embryo
294 inside the eggshell around the time of hatching, when the hatching glands make this narrow
295 belt in the yolk sac starting just caudal to the ear (Fig. 1A). At this stage the olfactory bulbs,
296 the unpigmented eyes, the developing brain, the lateral neuromasts and the ears can be seen
297 (Fig. 1C-D). A lateral view of a hatching embryo leaving the eggshell reveals the hatching
298 glands as a ring in the frontal part of the yolk sac showing the restricted digestion of the
299 eggshell (Fig. 1B). In our broad search for photoreceptive elements in the developing halibut
300 embryo we have earlier identified several melanopsins (Eilertsen et al., 2014) and we here
301 report an additional nonvisual opsin, VA opsin. Phylogenetic maximum likelihood analysis
302 verifies that this VA opsin branch together with other VA opsins (data not shown). Our ISH
303 results have detected a ball-shaped cluster of cells in the hindbrain of special interest,
304 expressing both VA opsin (Fig. 1E) and melanopsin (*opn4m3*) (Fig. 1F) around hatching. The
305 expression is seen bilaterally at the level of the lateral neuromasts, most likely in the second
306 rhombomere, caudal to the midbrain-hindbrain boundary. In addition, an oblique band at the

307 level of the ears, most likely in the fourth rhombomere, is seen for both genes, with strong
308 distinct expression of melanopsin. Nissl staining and ISH with VA opsin probe was done on
309 parallel sections and Fig. 1G-H show transversal sections and Fig. 1I-J show horizontal
310 sections through the hindbrain. The transversal sections show how the hindbrain cluster is
311 located in ventral parts of the hindbrain and the neuromast can be seen in the same section.
312 The horizontal sections reveal the location related to the midbrain-hindbrain boundary and in
313 addition, a positive cell of the oblique band is shown. To verify that the c-opsin homologue
314 VA opsin and the r-opsin homologue melanopsin are expressed in the same cells, fluorescent
315 double labelling ISH was done (Fig. 2A-F). Confocal imaging of a whole embryo showed that
316 the two genes are expressed in the same cluster in the hindbrain (Fig. 2A-C). A sagittal
317 section through the hindbrain cluster showed that VA opsin and melanopsin have overlapping
318 expression within the same cells of the aggregated cluster (Fig. 2D-F), with some cells in the
319 aggregated cluster just expressing one of the opsins (data not shown). The expression pattern
320 of the two genes has been analyzed around hatching (Fig. 2G-M) and show differences during
321 development of the hindbrain cluster. At 10 dpf VA opsin positive cells are visible in the
322 cluster (Fig. 2G) and at 13 dpf the expression is even more aggregated (Fig. 2H). After
323 hatching, at 17 dpf the expression is weaker and the VA opsin expression is disintegrated
324 (Fig. 2I) and this is even more apparent at 19 dpf where only a few cells are expressing VA
325 opsin (Fig. 2J). The mammalian-like melanopsin (*opn4m3*) is expressed in an aggregated
326 cluster already at 9 dpf (Fig. 2K) but at 13 dpf the melanopsin expression has started to scatter
327 (Fig. 2L). At 17 dpf the ball-shaped expression has disappeared from the neuronal cluster
328 (Fig. 2M).

329

330 **The hindbrain cluster is imbedded in a neuronal network projecting to the hatching**
331 **glands.** Newly differentiated neurons and axonal pathways were marked by antibody against
332 acetylated alpha tubulin to study the neuronal networks in the hindbrain in relation to the
333 bilateral nonvisual opsin expressing cluster (shown by ISH of VA opsin) (Fig. 3). Analyzing
334 the neuronal network of the embryo, it appears that fibers course along the yolk sac and
335 innervate the hatching gland cells (Fig. 3A, C, E). A close look on the hatching glands (Fig.
336 3B) and a curved fiber (Fig. 3D) show the close connection (Fig. 3F). Analyzing the VA opsin
337 expressing cells in the hindbrain clusters at 13 dpf (Fig. 3G) and the neuronal network (Fig.
338 3H) demonstrates the localization of the hindbrain clusters in relation to the fibers (Fig. 3I).
339 Further, confocal imaging of acetylated alpha tubulin demonstrates the neuronal network in
340 more detail (Fig. 3J-M), with an overview in Fig. 3J and with focus on the lateral fiber in Fig.

341 3K-L and the neuronal network of the hindbrain in Fig. 3M. Fig. 3K shows that the fiber
342 (probably the trigeminal sensory axon bundle) bends laterally anterior to the neuromast and
343 splits. Part of the fiber bundle proceeds lateral and exits the brain while others continue
344 dorsorostrally in the brain. Higher magnification and rotated view of the fiber (Fig. 3L) shows
345 the split and fiber extension out in the yolk sac. (See also Supplementary Figure 4 for a movie
346 of the 3D projection in Fig. 3K.) The neuronal network in the hindbrain (Fig. 3M) reveals that
347 the fiber coursing out in the yolk sac is lateral and located more dorsally. (See Supplementary
348 Figure 5 for a movie of the different focal levels in Fig. 3M.) Higher magnification of the
349 pictures in Fig. 3G-I shows the hindbrain cluster (Fig. 3N) and the fibers (Fig. 3P) on one side
350 of the embryo and a combination of the pictures illustrates how the fibers connected to the
351 hindbrain cluster proceed laterally to exit the brain just anterior to the neuromast (Fig. 3R). By
352 confocal imaging the connection between the VA opsin cluster (Fig. 3O) and the fibers (Fig.
353 3Q) is visualized in detail and the hindbrain cluster appears to be imbedded in a neuronal
354 network reaching the hatching glands (Fig. 3S).

355

356 **Dark-induced hatching of photo-arrested eggs gives *c-fos* activation in the hindbrain**
357 **and in hatching glands.** Neuronal activation in dark-induced hatching after photo-arrest was
358 analyzed by expression studies of the immediate early gene *c-fos*. Five eggs (18 dpf) per dark
359 stimulation (2, 10, 20, 30, 40, 60 and 120 minutes) were analyzed and all sampling points
360 except the 120 minutes showed the same expression pattern as the control (5 eggs analyzed)
361 incubated in light (data not shown). In contrast, at the sampling point 120 minutes expression
362 of *c-fos* was apparent in the hindbrain and in the hatching glands of all larvae studied (Fig. 4).
363 A picture of the yolk sac and hatching glands of an embryo sampled at 120 minutes shows the
364 *c-fos* expression in the ring of hatching glands (Fig. 4A) and a high magnification reveals the
365 distribution of *c-fos* expression in single hatching gland cells (Fig. 4B). Figure 4C shows VA
366 opsin expression in the hindbrain at the same developmental stage as the study with photo-
367 arrested eggs. At the sampling point 120 minutes, *c-fos* expression is detected in
368 telencephalon, midbrain and hindbrain (Fig. 4D). The expression in the hindbrain is a bilateral
369 ball-shaped cluster of cells resembling the morphology of the photosensitive hindbrain cluster
370 (Fig. 4D). In the light control, *c-fos* is expressed in a similar pattern in the telencephalon and
371 midbrain as the 120 minutes sampled eggs, but no expression is detected in the hindbrain (Fig.
372 4E). Fluorescent double labelling ISH in a 120 minutes sampled embryo shows that VA opsin
373 (Fig. 4F, G) and *c-fos* (Fig. 4H, I) are expressed in the same bilateral hindbrain cluster (Fig.
374 4J, K) in all the embryos studied.

375 **Discussion**

376 We present a unique study that combines the characterization of deep brain photoreceptor
377 cells and functional neuronal activation during hatching of Atlantic halibut eggs. Embryos of
378 halibut hatch at an early developmental stage when the eyes are not functional, yet the
379 development of deep brain nonvisual systems is advanced. This gives a special combination
380 of a nonvisual system, simple neuronal wiring and a light controlled hatching process. Our
381 findings suggest that hatching is under direct control of transient deep brain photoreceptor
382 cells expressing dual photopigments. These results allow the speculation that transient opsin
383 expression may be important to regulate other life history transition events as well.

384

385 **Transient photoreceptive hindbrain cluster and connections to the hatching glands.** In
386 our previous studies on Atlantic halibut (Eilertsen et al., 2014) we have described the early
387 complexity of melanopsins in deep brain photoreceptor cells in the hatching embryo, where
388 we found a bilateral ball-shaped hindbrain cluster expressing *opn4m3*. Remarkably, we found
389 that both types, VA opsin and *opn4m3*, are transiently expressed in this hindbrain cluster (Fig.
390 1 and 2). Previous studies have indicated a close overlap between VA opsin and melanopsin
391 expression (Bellingham et al., 2002; Jenkins et al., 2003; Sandbakken et al., 2012) or between
392 melanopsin and visual opsins (Davies et al., 2011). Here we show for the first time by
393 fluorescent double labelling ISH that these two opsins, originating from evolutionary distinct
394 heritages, c-opsin and r-opsin, are in fact expressed in the same cells. Earlier, it has been
395 shown that a marine invertebrate in the *Annelida* phylum, *Platynereis dumerilii* co-expresses
396 two opsins of different heritage, the r-opsin and the Go-opsin (Guehmann et al., 2015).
397 Recently, a marine mollusk, *Leptochiton asellus*, is found to co-express a newly discovered
398 xenopsin with r-opsin in a photoreceptor cell having both microvilli and cilia (Vocking et al.,
399 2017). Analyzing the dynamics of the hindbrain cluster, we found that opsins expressions are
400 transient with extensive distributions of both genes before hatching (Fig. 2). After hatching,
401 the expression of VA opsin and melanopsin in the developing cluster scatters and disappears
402 within a few days, indicating that one function of the hindbrain cluster is related to this early
403 life history transition. We further demonstrate that the hindbrain cluster is imbedded in a
404 neuronal network of fibers that extend into the yolk sac (Fig. 3). There exists a connection
405 between the photosensitive hindbrain cluster and the region of hatching glands in the yolk sac,
406 suggesting that the fibers provide a signal to the hatching glands. In addition, we observe no
407 RNA expression of visual opsins, melanopsins, exorhodopsin and VA opsin in the narrow belt

408 of hatching gland cells (data not shown), indicating that there is no direct photoreception
409 mediated by these opsin families in the hatching glands.

410

411 **Neural activity in the hindbrain cluster and hatching.** Light serves as a natural cue for
412 hatching in halibut eggs, and light synchronize hatching in such a way that it occurs at the
413 first night after the embryos have reached the developmental competency before hatching
414 (Helvik and Walther, 1992). Recently light-regulated hatching has also been demonstrated in
415 zebrafish and Senegalese sole (Villamizar et al., 2012; Villamizar et al., 2013). The
416 responsible photoreceptor cells and the mechanisms for regulating hatching have so far not
417 been elucidated. Our results in halibut show however that the immediate early gene *c-fos* is
418 expressed in the hindbrain cluster and hatching glands in a study with dark-induced hatching
419 after photo-arrest (Fig. 4). The expression of *c-fos* is activated rapidly and transiently in
420 response to a variety of stimuli such as growth factor stimulation and stimulation of nerve
421 cells (Bullitt, 1990; Sheng and Greenberg, 1990). Our results show expression of *c-fos* 120
422 minutes after the photo-arrested eggs were transferred to darkness. Although not shown
423 directly, these results indicate that darkness stimulates neural activity that induces hatching,
424 implying that light exerts inhibitory influences on melanopsin- and VA opsin-expressing
425 cells. Our data also suggest that the bilateral photosensitive hindbrain cluster mediates the
426 signal to the hatching glands, through the neuronal network with fibers out in the yolk sac. In
427 addition, even though the pineal organ has been suggested to be important in perceiving and
428 mediating photic information in the hatching process (Forsell et al., 1997) and has been
429 shown to express nonvisual opsins at the stage of hatching (Eilertsen et al., 2014), no *c-fos*
430 activation was detected in the pineal organ here.

431

432 **Dynamics of the dual photoreceptor cells in the hindbrain cluster and hatching.** The
433 melanopsin expression fades already prior to hatching in the hindbrain cluster (Fig. 2). A few
434 days after the natural hatching point, the melanopsin expression has disappeared while the VA
435 opsin expression persists a little longer. Evolutionarily, melanopsin and VA opsin are
436 believed to belong to different classes of photoreceptor pigments normally found in
437 rhabdomeric and ciliary photoreceptor cells and the phototransduction cascades involved are
438 thought to involve different machinery resulting in depolarization or hyperpolarization,
439 respectively (Arendt, 2003; Nilsson, 2004). Chromatic antagonism with a hyperpolarizing
440 light response sensitive to blue light (pinopsin) and a depolarizing light response sensitive to
441 green light (parietopsin) has been described in the parietal-eye photoreceptor cells of lizard,

442 but in contrast to melanopsin and VA opsin they both belong to the same class of
443 photopigments (Solessio and Engbretson, 1993; Su et al., 2006). However, they involve the
444 same phototransduction cascade leading to an antagonistic response employing different G
445 proteins (Su et al., 2006). In contrast, hyperpolarization response is not detected in the
446 rhabdomic adult eye of the invertebrate annelid *Platynereis* where Go-opsin is co-expressed
447 with two r-opsins. It has been suggested that Go-opsin does not antagonize the depolarization
448 response of r-opsins in the *Platynereis* eye (Guehmann et al., 2015). It is unknown how the
449 phototransduction cascade will function in the dual photoreceptor cluster of halibut expressing
450 both hyperpolarizing and depolarizing opsin types. One may speculate if light activates both
451 opsin types and balance the membrane potential so that the net charge is unchanged, leaving
452 the cell in a resting state. Fading of melanopsin at the time of hatching may allow a VA opsin-
453 driven cascade. It is conceivable that under the light the activation of the VA opsin
454 hyperpolarizes the photoreceptors and inhibits hatching. Shifting to darkness, the VA
455 hyperpolarized cells will be depolarized due to the dark current, giving a change in the
456 membrane potential allowing an activation of the hatching glands. The developmentally timed
457 down-regulation of melanopsin may therefore contribute to refining the time of hatching.

458

459 **Hatching, a direct brain photoreceptive control process.** Recently the hindbrain was for
460 the first time demonstrated to be responsible for a light-sensing behavior in vertebrates. The
461 caudal hindbrain of zebrafish was shown to drive series of robust and reproducible motor
462 behaviors as a response to visual wavelengths of light (Kokel et al., 2013). Here we suggest
463 that also the rostral hindbrain is involved in light-sensing behaviors in vertebrates. Our results
464 indicate that the environmental light is detected directly in the hindbrain providing behavioral
465 and physiological functions driven by neural activity. In zebrafish, the response was shown to
466 be dependent of the synthesis of 11-*cis* retinal, while the responsible opsin still needs to be
467 elucidated (Kokel et al., 2013). Our results show that the bilateral cluster of cells in the rostral
468 hindbrain expresses both VA opsin and melanopsin, giving the first indications of responsible
469 opsins in the hindbrain. Further, we can indicate the neuronal identity of the hindbrain cluster
470 based on the indicated location in the second rhombomere (Fig. 1) and confocal images of the
471 acetylated alpha tubulin (Fig. 3J-M). The location in the second rhombomere is relative lateral
472 (Fig. 1G-J) and corresponds with the location of the rostral trigeminal motor neuron (nVa)
473 located in the second rhombomere of zebrafish (Chandrasekhar et al., 1997; Higashijima et
474 al., 2000). In zebrafish where the neuronal network of the hindbrain is described in more
475 detail, the efferent axon of the nV is demonstrated to join the afferent trigeminal sensory axon

476 bundle, that turns rostrally and exits the hindbrain in rhombomere 2 (Chandrasekhar et
477 al., 1997). Unusual afferent innervations by the trigeminal ganglion have also been observed
478 in transient glands in other fishes and in amphibians (Roberts and Blight, 1975; Honore and
479 HemmatiBrivanlou, 1996; Pottin et al., 2010). In fish, it has been suggested that the axonal
480 guidance cues probably are provided by the target themselves and both the glands and the
481 fibers have a parallel transient nature related to their function early in development (Pottin et
482 al., 2010). The exact nature of the neuronal regulation of hatching and how photoreceptive
483 neurons, motor neurons and sensory neurons interact to control hatching, are open for further
484 investigations.

485

486 **Transient photoreceptors may regulate life history transitions.** Examples of temporary
487 photoreceptor cells are almost lacking in the literature but studies in invertebrates show that
488 larval eyes degrade during metamorphosis when the adult eyes start to form (Rhode, 1993;
489 Yamaguchi and Seaver, 2013). In sea lamprey reduced dermal photosensitivity has been
490 shown to reflect life history dependent changes in habitat and behavior (Binder et al., 2013),
491 but the responsible cells and photopigments have not been detected. Here we demonstrate a
492 transient photoreceptive cluster of cells in the hindbrain of halibut near hatching and we
493 indicate that this cluster is permissive for this early life history transition. Our results illustrate
494 neurons whose photoreceptive activities are not fixed throughout life and that they can be
495 developmentally regulated toward a biological event. The finding supports a gene-expression
496 signature study of life history transitions in Atlantic salmon where the gene expression of a
497 rod-like opsin (most equivalent to exorhodopsin) is shown to be up- and down-regulated at
498 different life history stages (Aubin-Horth et al., 2009). The concept of transient light
499 sensitivity to target critical aspect of life opens for investigation of other biological events to
500 be regulated by specific transient nonvisual photoreceptor systems.

501

502 **Acknowledgements**

503 We thank Rolf B. Edvardsen at the Institute of Marine Research for providing the sequence of
504 *c-fos* and for validating our VA opsin sequence data by searching the Atlantic halibut genome.
505 Thanks to Sterling White Halibut for founding the Atlantic halibut genome sequencing and
506 Ragnfrid Mangor-Jensen at the Austevoll Aquaculture Research Station for providing Atlantic
507 halibut eggs. The confocal imaging of acetylated alpha tubulin was performed at the
508 Molecular Imaging Center (MIC) and was thus supported by the Department of Biomedicine
509 and the Faculty of Medicine and Dentistry, at the University of Bergen, and its partners.

510 **References**

- 511 Arendt D. 2003. Evolution of eyes and photoreceptor cell types. *Int J Dev Biol* 47(7-8):563-
512 571.
- 513 Aubin-Horth N, Letcher BH, Hofmann HA. 2009. Gene-expression signatures of Atlantic
514 salmon's plastic life cycle. *Gen Comp Endocrinol* 163(3):278-284.
- 515 Bellingham J, Whitmore D, Philp AR, Wells DJ, Foster RG. 2002. Zebrafish melanopsin:
516 isolation, tissue localisation and phylogenetic position. *Brain Res Mol Brain Res*
517 107(2):128-136.
- 518 Binder TR, McDonald DG, Wilkie MP. 2013. Reduced dermal photosensitivity in juvenile
519 sea lampreys (*Petromyzon marinus*) reflects life-history-dependent changes in habitat
520 and behaviour. *Can J Zool* 91(9):635-639.
- 521 Bullitt E. 1990. Expression of C-fos-like
522 protein as a marker for neuronal-activity following noxious-stimulation in the rat.
Journal of Comparative Neurology 296(4):517-530.
- 523 Burge C, Karlin S. 1997. Prediction of complete gene structures in human genomic DNA. *J*
524 *Mol Biol* 268(1):78-94.
- 525 Chandrasekhar A, Moens CB, Warren JT, Kimmel CB, Kuwada JY. 1997. Development of
526 branchiomotor neurons in zebrafish. *Development* 124(13):2633-2644.
- 527 Chitnis AB, Kuwada JY. 1990. Axonogenesis in the brain of zebrafish embryos. *J Neurosci*
528 10(6):1892-1905.
- 529 Davies WIL, Tamai TK, Zhen L, Fu JK, Rihel J, Foster RG, Whitmore D, Hankins MW.
530 2015. An extended family of novel vertebrate photopigments is widely expressed and
531 displays a diversity of function. *Genome Res* 25(11):1666-1679.
- 532 Davies WIL, Zheng L, Hughes S, Tamai TK, Turton M, Halford S, Foster RG, Whitmore D,
533 Hankins MW. 2011. Functional diversity of melanopsins and their global expression
534 in the teleost retina. *Cell Mol Life Sci* 68(24):4115-4132.
- 535 Davies WL, Hankins MW, Foster RG. 2010. Vertebrate ancient opsin and melanopsin:
536 divergent irradiance detectors. *Photoch Photobio Sci* 9(11):1444-1457.
- 537 Eilertsen M, Drivenes Ø, Edvardsen RB, Bradley CA, Ebbesson LOE, Helvik JV. 2014.
538 Exorhodopsin and melanopsin systems in the pineal complex and brain at early
539 developmental stages of Atlantic halibut (*Hippoglossus hippoglossus*). *Journal of*
540 *Comparative Neurology* 522(18):4003-4022.

541 Fernandes AM, Fero K, Arrenberg AB, Bergeron SA, Driever W, Burgess HA. 2012. Deep
542 brain photoreceptors control light-seeking behavior in zebrafish larvae. *Curr Biol*
543 22(21):2042-2047.

544 Fernandes AM, Fero K, Driever W, Burgess HA. 2013. Enlightening the brain: Linking deep
545 brain photoreception with behavior and physiology. *Bioessays* 35(9):775-779.

546 Fischer RM, Fontinha BM, Kirchmaier S, Steger J, Bloch S, Inoue D, Panda S, Rumpel S,
547 Tessmar-Raible K. 2013. Co-expression of VAL- and TMT-opsins uncovers ancient
548 photosensory interneurons and motoneurons in the vertebrate brain. *Plos Biol* 11(6).

549 Forsell J, Holmqvist B, Helvik JV, Ekström P. 1997. Role of the pineal organ in the
550 photoregulated hatching of the Atlantic halibut. *Int J Dev Biol* 41(4):591-595.

551 Guehmann M, Jia H, Randel N, Veraszto C, Bezares-Calderon LA, Michiels NK, Yokoyama
552 S, Jekely G. 2015. Spectral tuning of phototaxis by a Go-opsin in the rhabdomeric
553 eyes of *Platynereis*. *Curr Biol* 25(17):2265-2271.

554 Halford S, Pires SS, Turton M, Zheng L, Gonzalez-Menendez I, Davies WL, Peirson SN,
555 Garcia-Fernandez JM, Hankins MW, Foster RG. 2009. VA opsin-based
556 photoreceptors in the hypothalamus of birds. *Curr Biol* 19(16):1396-1402.

557 Haug T. 1990. Biology of the Atlantic halibut, *Hippoglossus hippoglossus* (L, 1758). *Adv*
558 *Mar Biol* 26:1-70.

559 Haug T, Kjørsvik E, Solemdal P. 1984. Vertical-distribution of Atlantic halibut
560 (*Hippoglossus-Hippoglossus*) eggs. *Can J Fish Aquat Sci* 41(5):798-804.

561 Helvik JV, Drivenes Ø, Naess TH, Fjose A, Seo HC. 2001. Molecular cloning and
562 characterization of five opsin genes from the marine flatfish Atlantic halibut
563 (*Hippoglossus hippoglossus*). *Visual Neurosci* 18(5):767-780.

564 Helvik JV, Oppen-Berntsen DO, Walther BT. 1991. The hatching mechanism in Atlantic
565 halibut (*Hippoglossus hippoglossus*). *Int J Dev Biol* 35(1):9-16.

566 Helvik JV, Walther BT. 1992. Photo-regulation of the hatching process of halibut
567 (*Hippoglossus hippoglossus*) eggs. *J Exp Zool* 263(2):204-209.

568 Helvik JV, Walther BT. 1993. Development of hatchability in halibut (*Hippoglossus*
569 *hippoglossus*) embryos. *Int J Dev Biol* 37(3):487-490.

570 Higashijima S, Hotta Y, Okamoto H. 2000. Visualization of cranial motor neurons in live
571 transgenic zebrafish expressing green fluorescent protein under the control of the *Islet-*
572 *1* promoter/enhancer. *J Neurosci* 20(1):206-218.

573 Honore E, HemmatiBrivanlou A. 1996. *In vivo* evidence for trigeminal nerve guidance by the
574 cement gland in *Xenopus*. *Dev Biol* 178(2):363-374.

575 Hunter PR, Nikolaou N, Odermatt B, Williams PR, Drescher U, Meyer MP. 2011.
576 Localization of Cadm2a and Cadm3 proteins during development of the zebrafish
577 nervous system. *J Comp Neurol* 519(11):2252-2270.

578 Jenkins A, Munoz M, Tarttelin EE, Bellingham J, Foster RG, Hankins MW. 2003. VA opsin,
579 melanopsin, and an inherent light response within retinal interneurons. *Curr Biol*
580 13(15):1269-1278.

581 Kojima D, Mano H, Fukada Y. 2000. Vertebrate ancient-long opsin: A green-sensitive
582 photoreceptive molecule present in zebrafish deep brain and retinal horizontal cells. *J*
583 *Neurosci* 20(8):2845-2851.

584 Kojima D, Torii M, Fukada Y, Dowling JE. 2008. Differential expression of duplicated VAL-
585 opsin genes in the developing zebrafish. *J Neurochem* 104(5):1364-1371.

586 Kokel D, Dunn TW, Ahrens MB, Alshut R, Cheung CY, Saint-Amant L, Bruni G, Mateus R,
587 van Ham TJ, Shiraki T, Fukada Y, Kojima D, Yeh JR, Mikut R, von Lintig J, Engert
588 F, Peterson RT. 2013. Identification of nonvisual photomotor response cells in the
589 vertebrate hindbrain. *J Neurosci* 33(9):3834-3843.

590 Kvenseth AM, Pittman K, Helvik JV. 1996. Eye development in Atlantic halibut
591 (*Hippoglossus hippoglossus*): Differentiation and development of the retina from early
592 yolk sac stages through metamorphosis. *Can J Fish Aquat Sci* 53(11):2524-2532.

593 Ledizet M, Piperno G. 1991. Detection of acetylated alpha-tubulin by specific antibodies.
594 *Method Enzymol* 196:264-274.

595 Liu JX, Lessman CA. 2007. Soluble tubulin complexes, gamma-tubulin, and their changing
596 distribution in the zebrafish (*Danio rerio*) ovary, oocyte and embryo. *Comp Biochem*
597 *Physiol B-Biochem Mol Biol* 147(1):56-73.

598 Matos-Cruz V, Blasic J, Nickle B,
599 Robinson PR, Hattar S, Halpern ME. 2011. Unexpected diversity and photoperiod
dependence of the zebrafish melanopsin system. *Plos One* 6(9).

600 Nakane Y, Ikegami K, Iigo M, Ono H, Takeda K, Takahashi D, Uesaka M, Kimijima M,
601 Hashimoto R, Arai N, Suga T, Kosuge K, Abe T, Maeda R, Senga T, Amiya N,
602 Azuma T, Amano M, Abe H, Yamamoto N, Yoshimura T. 2013. The saccus
603 vasculosus of fish is a sensor of seasonal changes in day length. *Nat Commun* 4:7.

604 Nilsson DE. 2004. Eye evolution: a question of genetic promiscuity. *Curr Opin Neurobiol*
605 14(4):407-414.

606 Peirson SN, Halford S, Foster RG. 2009. The evolution of irradiance detection: melanopsin
607 and the non-visual opsins. *Philos T R Soc B* 364(1531):2849-2865.

608 Pottin K, Hyacinthe C, Retaux S. 2010. Conservation, development, and function of a cement
609 gland-like structure in the fish *Astyanax mexicanus*. P Natl Acad Sci USA
610 107(40):17256-17261.

611 Rhode B. 1993. Larval and adult eyes in *Capitella spec. I* (Annelida, Polychaeta) J Morphol
612 217(3):327-335.

613 Roberts A, Blight AR. 1975. Anatomy, physiology and behavioral role of sensory nerve-
614 endings in cement gland of embryonic *Xenopus*. Proceedings of the Royal Society
615 Series B-Biological Sciences 192(1106):111-127.

616 Sandbakken M, Ebbesson L, Stefansson S, Helvik JV. 2012. Isolation and characterization of
617 melanopsin photoreceptors of Atlantic salmon (*Salmo salar*). J Comp Neurol
618 520(16):3727-3744.

619 Sheng M, Greenberg ME. 1990. The regulation and function of *c-fos* and other immediate
620 early genes in the nervous-system. Neuron 4(4):477-485.

621 Solessio E, Engbretson GA. 1993. Antagonistic chromatic mechanisms in photoreceptors of
622 the parietal eye of lizards. Nature 364(6436):442-445.

623 Su CY, Luo DG, Terakita A, Shichida Y, Liao HW, Kazmi MA, Sakmar TP, Yau KW. 2006.
624 Parietal-eye phototransduction components and their potential evolutionary
625 implications. Science 311(5767):1617-1621.

626 Thisse C, Thisse B. 2008. High-resolution *in situ* hybridization to whole-mount zebrafish
627 embryos. Nat Protoc 3(1):59-69.

628 Verpy E, Leibovici M, Michalski N, Goodyear RJ, Houdon C, Weil D, Richardson GP, Petit
629 C. 2011. Stereocilin connects outer hair cell stereocilia to one another and to the
630 tectorial membrane. J Comp Neurol 519(2):194-210.

631 Villamizar N, Blanco-Vives B, Oliveira C, Dinis MT, Di Rosa V, Negrini P, Bertolucci C,
632 Sanchez-Vazquez FJ. 2013. Circadian rhythms of embryonic development and
633 hatching in fish: A comparative study of zebrafish (diurnal), Senegalese sole
634 (nocturnal), and Somalian cavefish (blind). Chronobiol Int 30(7):889-900.

635 Villamizar N, Ribas L, Piferrer F, Vera LM, Sanchez-Vazquez FJ. 2012. Impact of daily
636 thermocycles on hatching rhythms, larval performance and sex differentiation of
637 zebrafish. Plos One 7(12).

638 Vocking O, Kourtesis I, Tumu SC, Hausen H. 2017. Co-expression of xenopsin and
639 rhabdomeric opsin in photoreceptors bearing microvilli and cilia. eLife 6.

640 Yamaguchi E, Seaver EC. 2013. The importance of larval eyes in the polychaete *Capitella*
641 *teleta*: effects of larval eye deletion on formation of the adult eye. *Invertebr Biol*
642 132(4):352-367.

643

644

645

646

647

648

649

650

651

652

653

654

655

656

657

658

659

660

661

662

663

664

665

666

667

668

669

670

671

672

673 **Table 1 Primers vertebrate ancient opsin**

Primer name	Sequence (5'-3')	Use
OpsinFw	AAGAAGYTCMGTCMACCTCTYAAYT	Degenerative primer
OpsinRv	GTTTCATGAAGACRTAGATDAYAGGGTTRTA	Degenerative primer
VAF1	CATCCGACCATCCAACCTCGAT	3'RACE
VAR1	TGATGTAGCTGTGAGCCGTCATG	5'RACE
VAF2	CCAAGACAGCCGCTGTCTACAA	Nested 3'RACE
VAR2	GTCAGGCTCACAGGTTGTTCCAATCTT	Nested 5'RACE

674

675 **Table 2 Sequence information**

Name	GenBank no.	cDNA length	predicted ORF	Predicted aa length	Binding site for the <i>in situ</i> probe (5'-3')	Probe length
<i>val</i>	KF941295	1743 bp	1164 bp	387 aa	102 - 1182 bp	1081 bp
<i>vas</i>	KF941296	1598 bp	987 bp	328 aa	102 - 1182 bp	1081 bp
<i>opn4m3short</i>	KF941290	1780 bp	1638 bp	545 aa	1 - 1089 bp	1089 bp
<i>opn4m3long</i>	KF941291	1846 bp	1704 bp	567 aa	1 - 1089 bp	1089 bp
<i>c-fos</i>	KF941297	1261 bp	1128 bp	375 aa	1 - 1261 bp	1261 bp

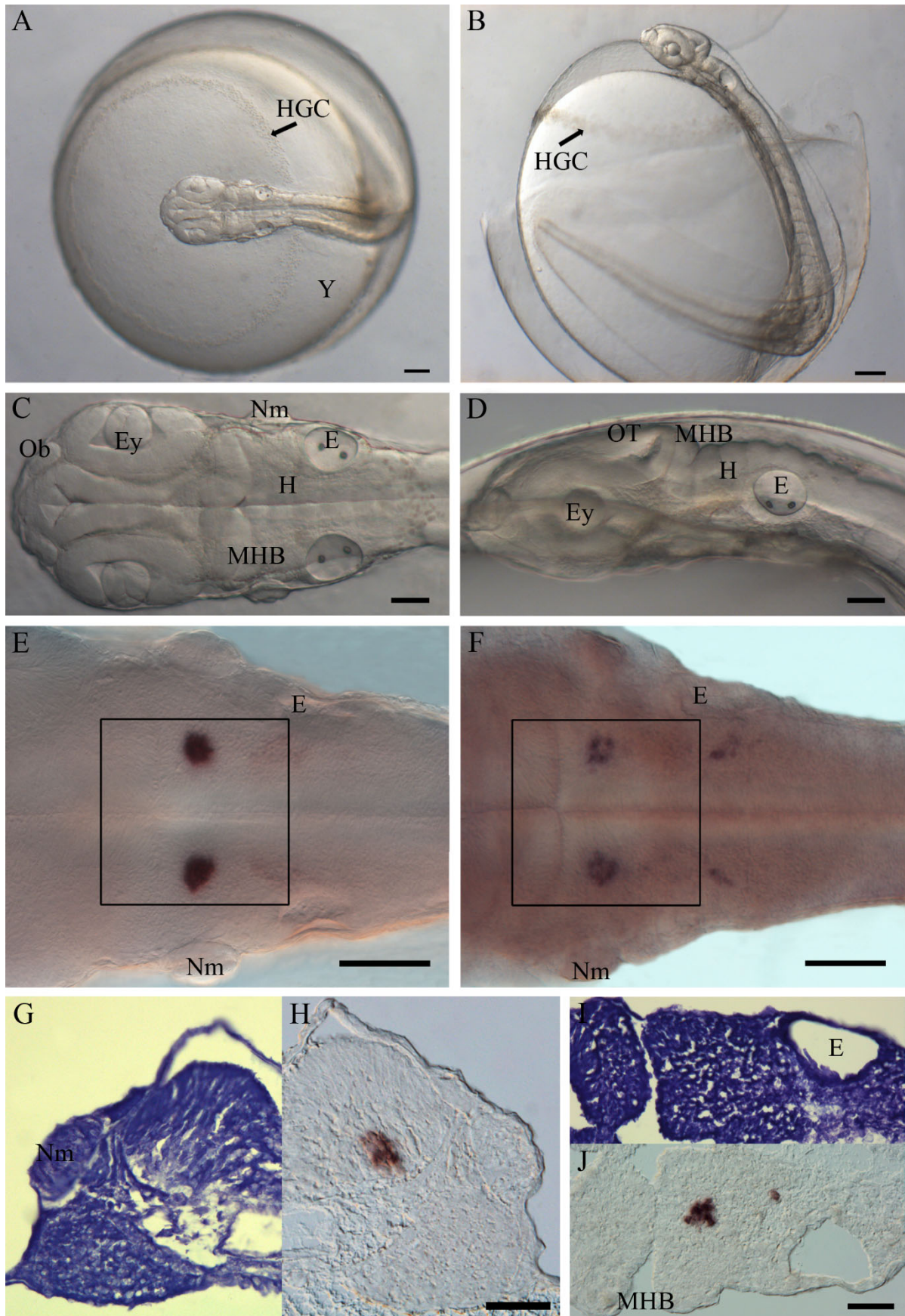
676

677 **Table 3 Antibodies**

Antibody	Immunogen	Manufacturer, host species, mono- vs. polyclonal, catalog number, RRIDs	Dilution
anti-acetylated tubulin	<i>Chlamydomonas axonemal</i> α -tubulin within four residues of acetylated Lys-40	Sigma-Aldrich (St. Louis, MO), Mouse monoclonal, IgG2b, #T7451, RRID: AB_609894	1:1,000
anti-digoxigenin conjugated with alkaline phosphatase, Fab fragments	digoxigenin (DIG)	Roche Diagnostics (Germany), Sheep polyclonal, #11093274910, RRID: AB_514497	1:2,000
anti-fluorescein conjugated with horse radish peroxidase, Fab fragments	fluorescein	Roche Diagnostics (Germany), Sheep polyclonal, #11426346910, RRID: AB_840257	1:400
anti-mouse IgG (H+L), CF TM 488A	mouse IgG (H+L)	Sigma-Aldrich (St. Louis, MO) Goat polyclonal, #SAB4600042, RRID: AB_2532075	1:100
anti-mouse IgG (H+L), CF TM 555	mouse IgG (H+L)	Sigma-Aldrich (St. Louis, MO) Goat polyclonal, #SAB4600066, RRID: AB_2336060	1:100

678

679

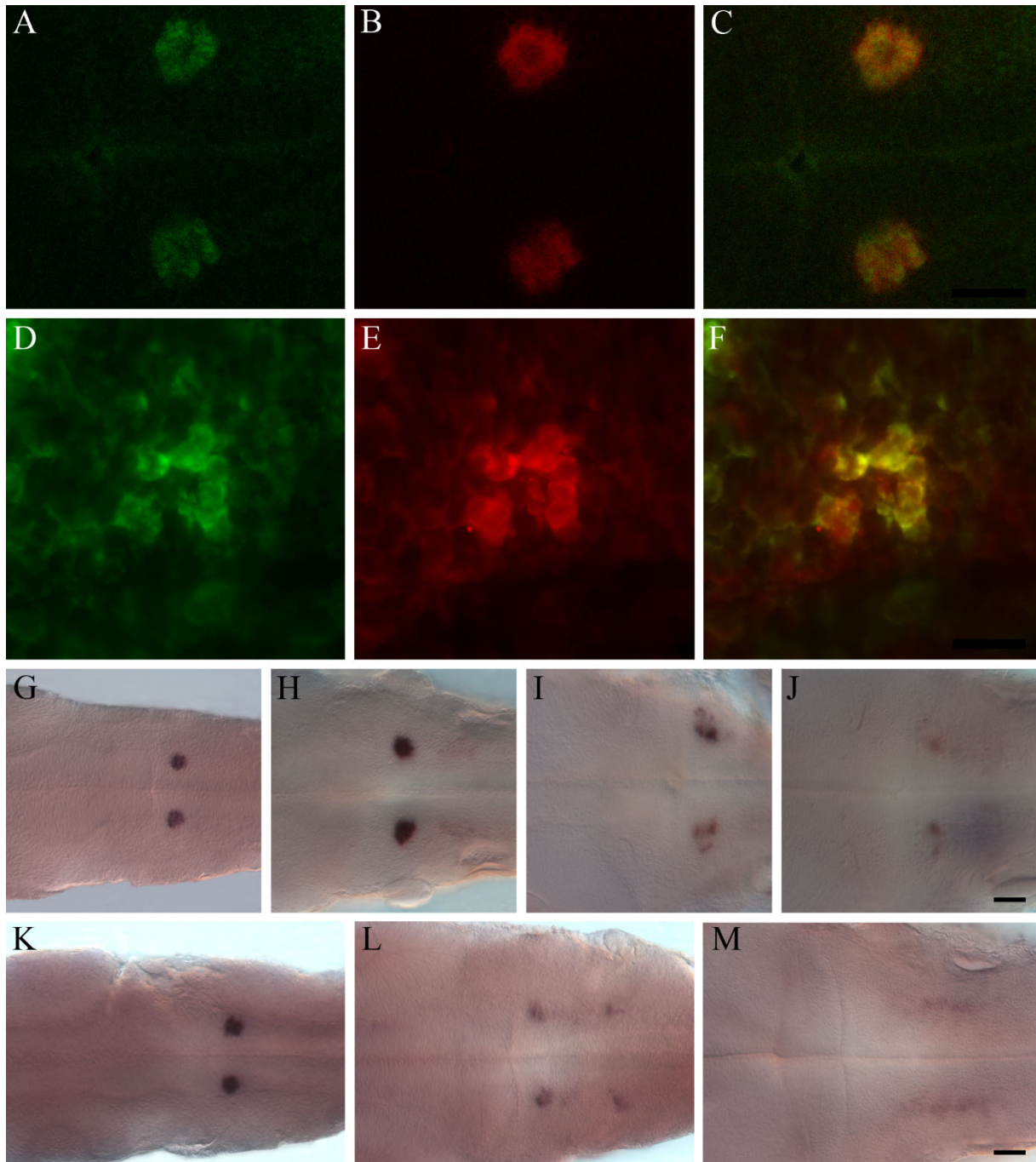


680

681 **Figure 1** The hatching Atlantic halibut, expression of nonvisual opsins in a bilateral hindbrain

682 cluster. **A:** A dorsal view of an embryo in the eggshell on the top of a huge yolk sac (Y) with

683 hatching glands cells (HGC) in a narrow belt, indicated by a black arrow. **B:** A hatching
684 embryo leaving the eggshell with the hatching glands in a frontal ring (black arrow) showing
685 the restricted digestion of the eggshell. **C:** Higher magnification of dorsal view in (**A**) shows
686 the olfactory bulb (Ob), eyes (Ey), midbrain-hindbrain boundary (MHB), hindbrain (H),
687 neuromasts (Nm) and ears (E). **D:** A lateral view shows the optic tectum (OT) and the
688 structures of the hindbrain including the MHB and the rhombomeres. **E, F:** Halibut embryos
689 with vertebrate ancient opsin (VA opsin) (**E**) and melanopsin (*opn4m3*) (**F**) expression in
690 bilateral ball-shaped clusters and oblique bands in the hindbrain at the stage of hatching. **G-J:**
691 Parallel transversal (**G-H**) and horizontal (**I-J**) sections showing Nissl-staining (**G, I**) and VA
692 opsin expression (**H, J**) of the hindbrain. Scale bars: 200 μm in A-B, 100 μm in C-F, 50 μm in
693 G-J.



694
 695 **Figure 2** Transient and dual expression of the nonvisual opsins in the hindbrain cluster. **A-C**:
 696 Confocal imaging of a whole embryo with VA opsin (**A**) and melanopsin (**B**) and the two
 697 genes together (**C**) show that the genes are expressed in the same cluster. **D-F**: Fluorescent
 698 microscopy of a sagittal section reveals that VA opsin (**D**) and melanopsin (**E**) are in the same
 699 cells in the cluster (**F**). **G-J**: Expression of VA opsin in the developing embryo around
 700 hatching. At 10 days post fertilization (dpf) VA opsin is expressed in the hindbrain cluster (**G**)
 701 and at 13 dpf the cluster is more condensed (**H**). After hatching at 17 dpf the VA opsin
 702 expressing cells scatter (**I**) and at 19 dpf only a few cells express VA opsin (**J**). **K-M**:
 703 Expression of melanopsin in the developing embryo around hatching. At 9 dpf melanopsin is

704 extensively expressed in the hindbrain cluster (**K**) but already at 13 dpf fewer cells in the
705 cluster express melanopsin (**L**). After hatching (17 dpf) no melanopsin positive cells are
706 observed in the hindbrain cluster (**M**). Scale bars: 50 μm in A-C and G-M, 20 μm in D-F.
707 (See Supplementary Figure 1 for magenta/green copy.)

708

709

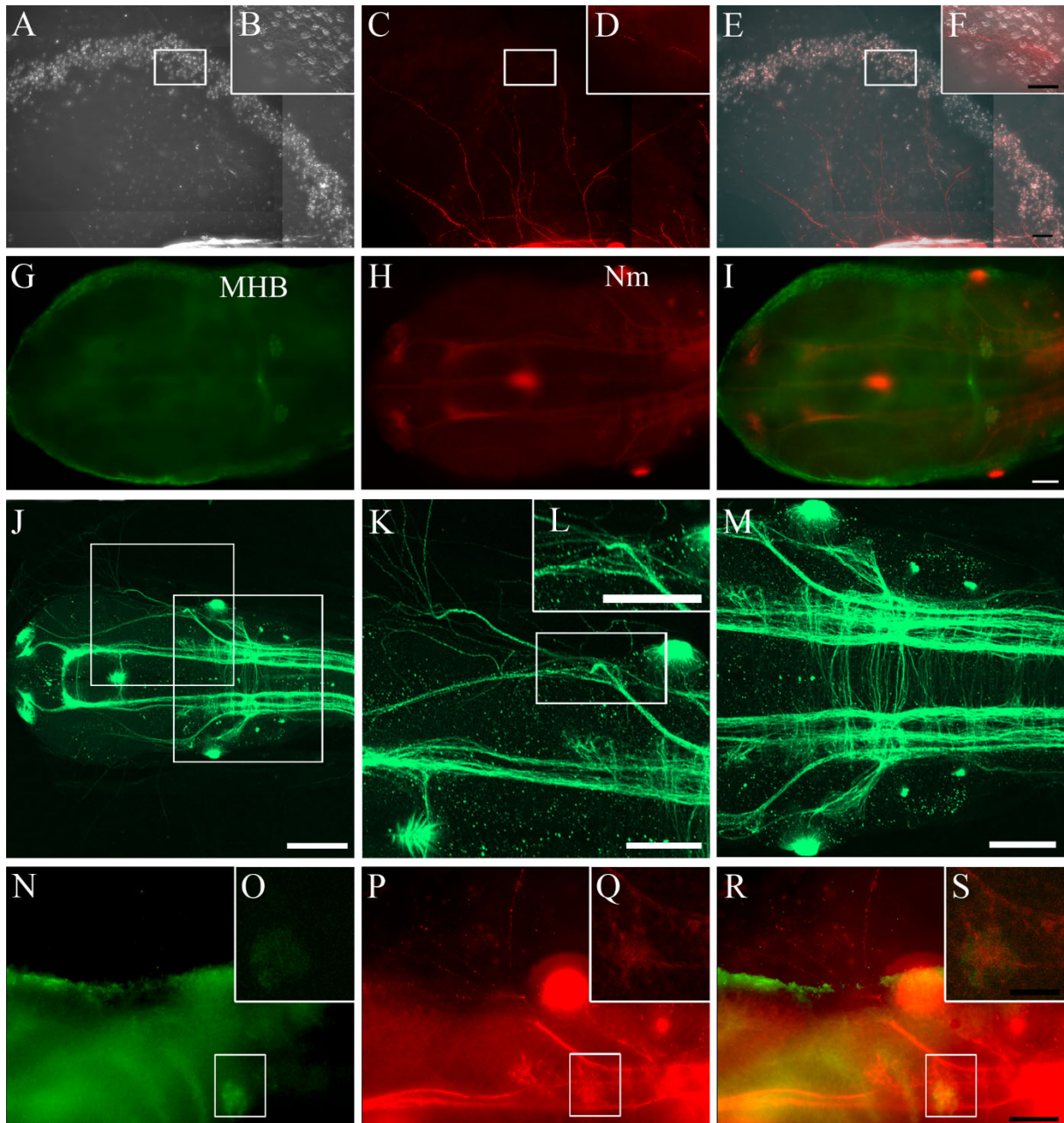
710

711

712

713

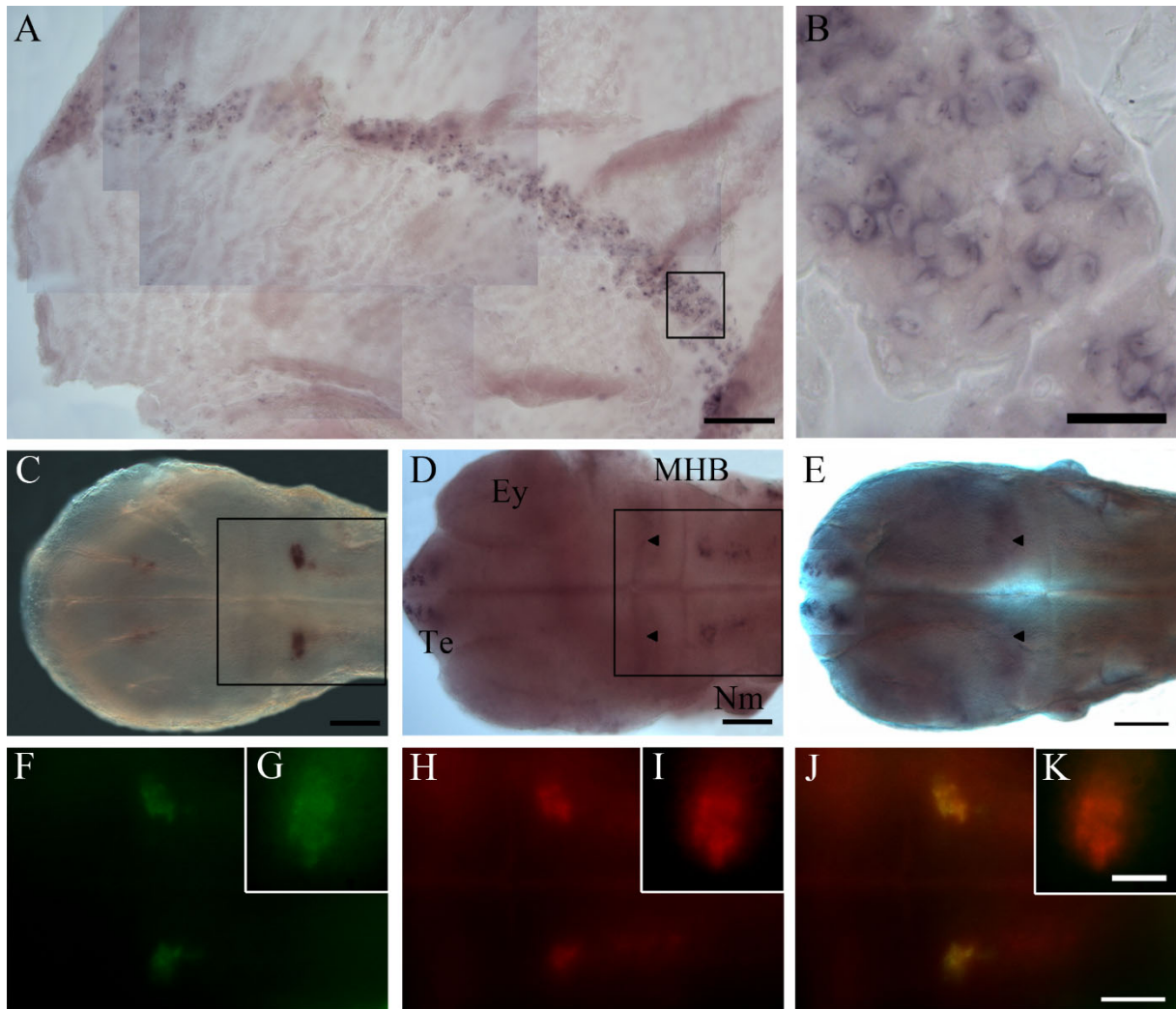
714



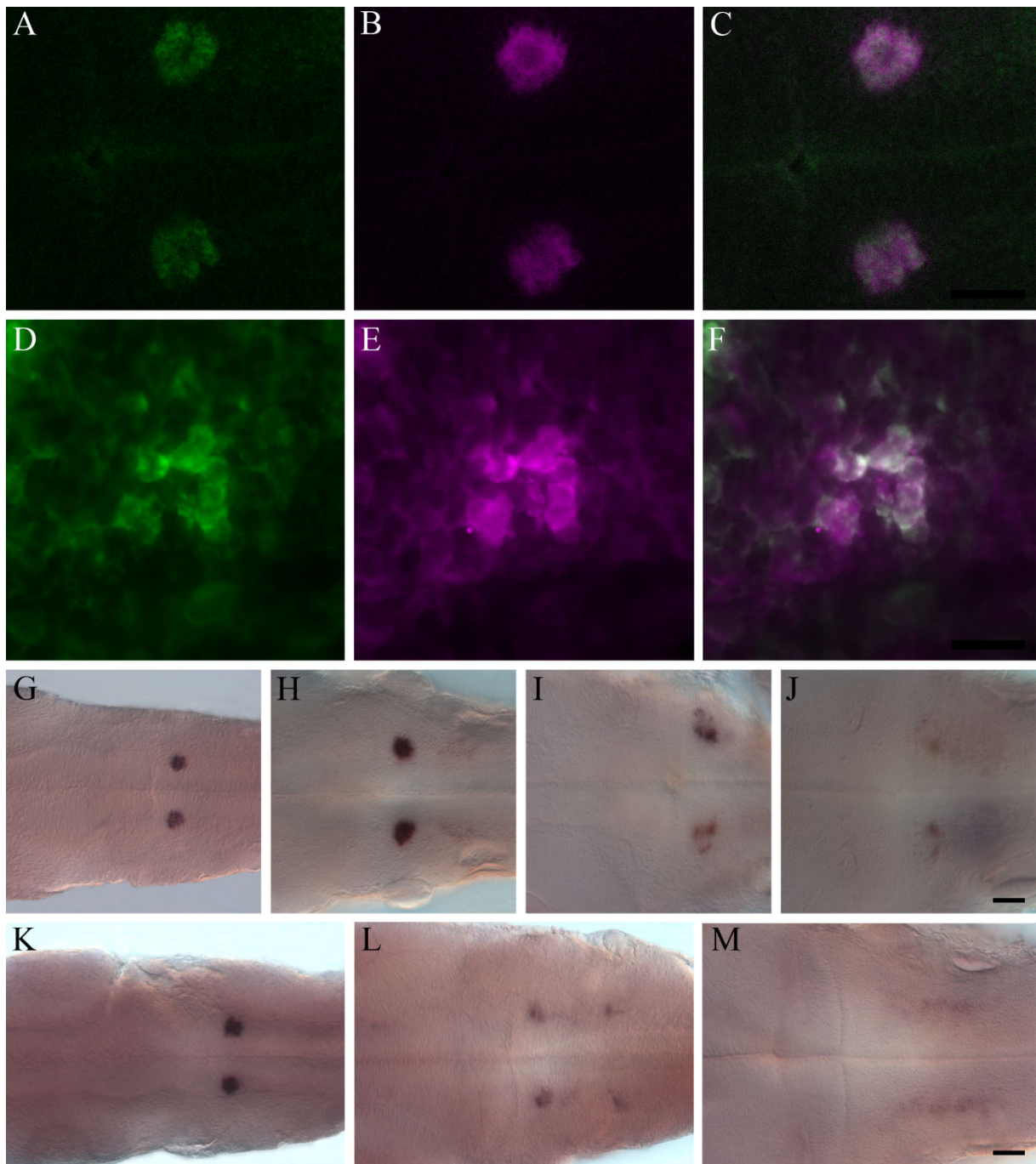
715

716 **Figure 3** The hindbrain cluster is imbedded in a neuronal network sending fibers out in the
 717 yolk sac, innervating the hatching gland cells. **A:** Assembly of dorsal view pictures of
 718 hatching glands at 13 days post fertilization (dpf) at one side of the embryo, high
 719 magnification of some hatching gland cells (**B**). **C:** Acetylated alpha tubulin illustrates the
 720 fibers coursing out in the yolk sac shown by the same collection of pictures as in (**A**), high
 721 magnification of a curved fiber (**D**). **E:** A combination of (**A**) and (**C**) shows how the
 722 widespread fibers innervate the hatching glands. **F:** (**B**) and (**D**) in combination show the
 723 close relation between the hatching glands and the curved fiber. **G:** Vertebrate ancient opsin
 724 (VA opsin) positive cells in the hindbrain at 13 dpf located caudal to the midbrain-hindbrain
 725 boundary (MHB). **H:** Newly differentiated neurons and axonal pathways in the same embryo

726 shown by acetylated alpha tubulin. **I:** A combination of VA opsin and acetylated alpha tubulin
727 picturing fibers nearby the hindbrain cluster bending at the level of the neuromasts. **J:**
728 Confocal image of acetylated alpha tubulin showing an overview of the forebrain, midbrain
729 and hindbrain. **K:** Higher magnification of the fiber coursing out of the brain (probably the
730 trigeminal sensory axon bundle) revealed by 3D projection. The picture reveals that the fiber
731 split and one of the fibers proceeds dorsorostrally in the brain while one fiber projects out in
732 the yolk and spreads as a fan. **L:** Focus on the fiber where it splits, with a rotated ventral view
733 of the 3D projection. **M:** Higher magnification of the neuronal network in the hindbrain
734 revealed by a 3D projection. The fiber bending lateral at the level of the neuromast is located
735 laterally. **N:** Focus on one of the VA opsin expressing hindbrain clusters and confocal
736 imaging of the cluster (**O**). **P:** Detail of the fibers proceeding laterally spreading out in the
737 yolk sac as a fan, confocal imaging (**Q**). **R:** The hindbrain cluster is imbedded in the network
738 sending fibers out in the yolk sac. **S:** A combination of the confocal images in (**O**) and (**Q**)
739 shows the connection between the hindbrain cluster and fibers. Scale bars: 200 μm in J, 100
740 μm in A, C, E, G-I, K-M, N, P, R, 50 μm in O, Q, S, 20 μm in B, D, F. Neuromast (Nm) (See
741 Supplementary Figure 2 for magenta/green copy and Supplementary Figure 4 and 5 for
742 movies of the confocal images of acetylated alpha tubulin.)

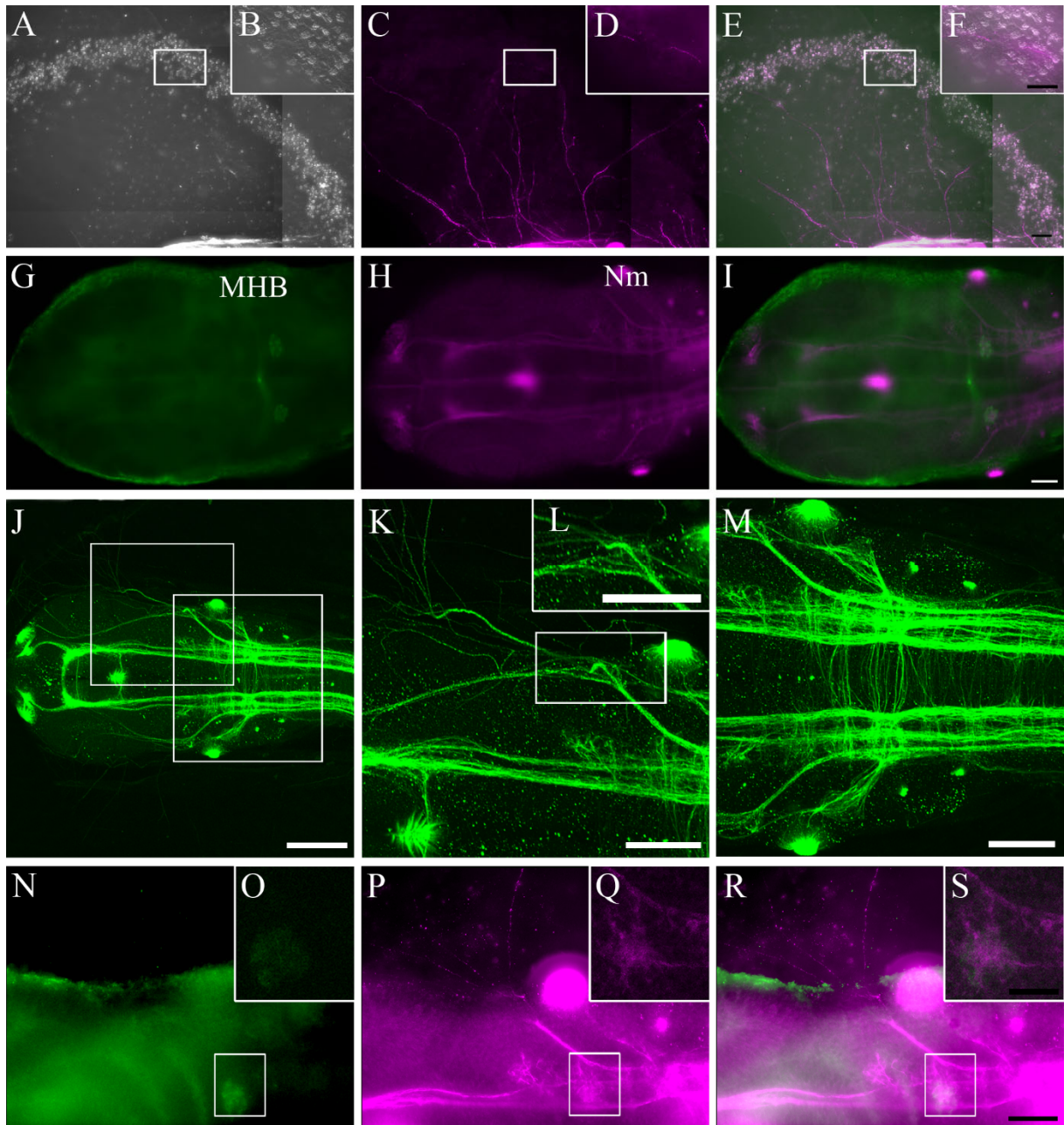


743
 744 **Figure 4** Transfer of photo-arrested eggs to darkness gives neural activation in the hindbrain
 745 cluster and hatching glands in the eggs sampled after 120 minutes. **A:** Pictures of the yolk sac
 746 and hatching glands of 120 minutes sampled embryo put together to illustrate the *c-fos*
 747 expression in the hatching glands. **B:** Detail of the hatching glands expressing *c-fos*. **C:**
 748 Vertebrate ancient opsin (VA opsin) in the hindbrain cluster at the same developmental stage
 749 as the study with dark-induced hatching after photo-arrest. **D:** At the sampling point 120
 750 minutes neural activation is shown by *c-fos* expression in the telencephalon (Te), midbrain
 751 (black arrowhead) and hindbrain. The hindbrain expression is caudal to the midbrain-
 752 hindbrain boundary (MHB) and at the level of the neuromast (Nm), most likely in the second
 753 rhombomere. **E:** Expression of *c-fos* in a control kept in light shows expression in
 754 telencephalon and midbrain (black arrowhead). **F-K** Fluorescent double labelling ISH of the
 755 120 minutes sampled embryo with VA opsin (**F-G**) and *c-fos* (**H-I**) shows that both are
 756 expressed in the hindbrain cluster (**J-K**). Scale bars: 100 μm in A, C-E, F, H, J, 50 μm in G, I,
 757 K, 20 μm in B. Eye (Ey) (See Supplementary Figure 3 for 1.)



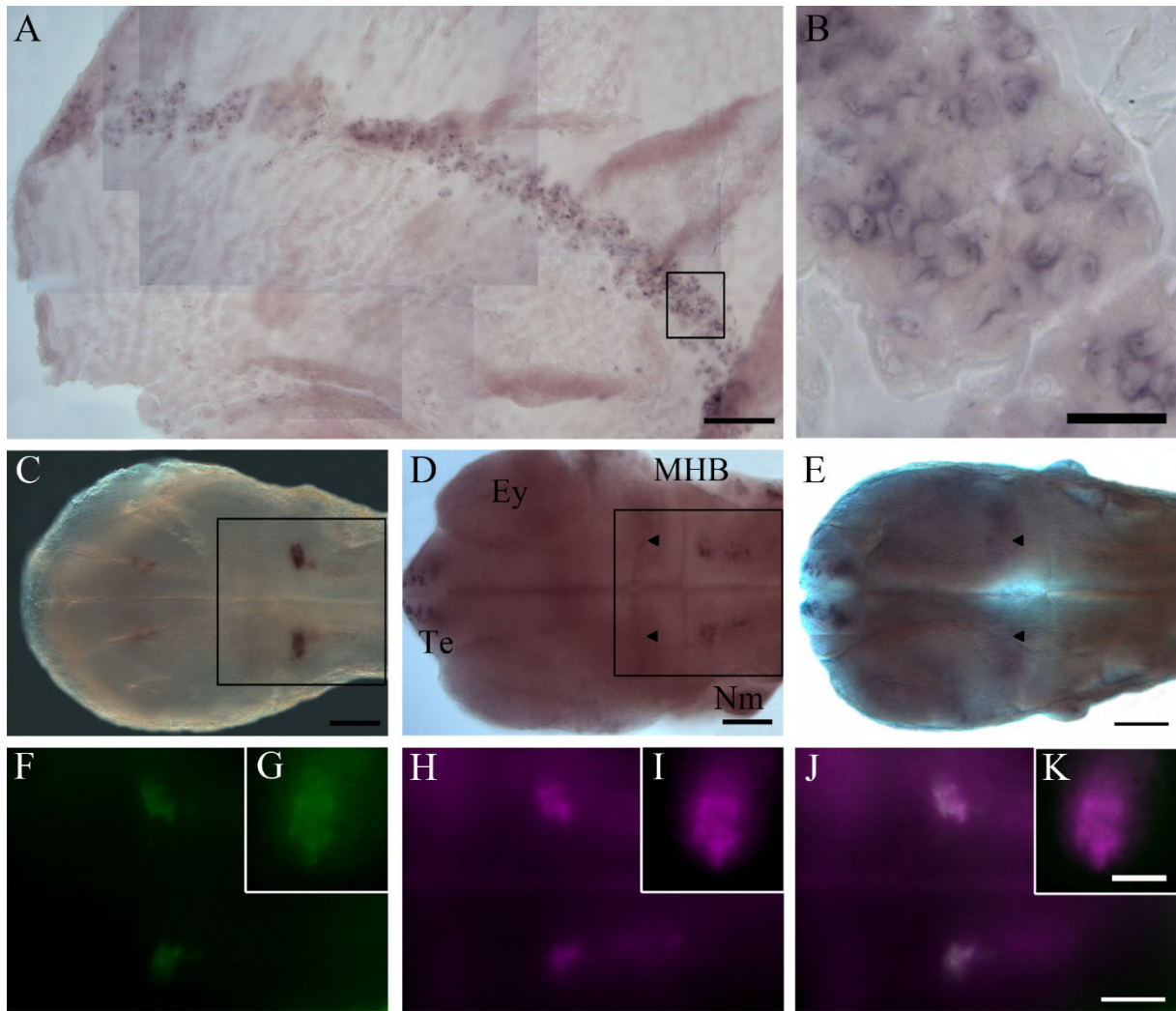
758

759 **Supplementary figure 1** (See Figure 2 for figure legend)



760

761 **Supplementary figure 2** (See Figure 3 for figure legend)



762
763
764
765

Supplementary figure 3 (See Figure 4 for figure legend)

766
767
768
769
770
771

Supplementary Figure 4 Movie of confocal images, view as Figure 3K. The movie is generated by merging a stack of pictures providing 3D projections that are set together as a movie. The movie illustrates the lateral fiber bundle that splits anterior to the neuromast where parts of the fibers course out in the yolk sac and others continue dorsorostrally in the brain.

772
773
774
775
776

Supplementary Figure 5 Movie of confocal images, view as Figure 3M. The movie is generated by pictures of different focal levels that are set together as a movie. The movie illustrates the neuronal network in the hindbrain of halibut, from a dorsal to ventral view, revealing that the lateral fiber bundle is located more dorsally.